BOHR International Journal of Biocomputing and Nano Technology
2022, Vol. 1, No. 1, pp. 1–8
https://doi.org/10.54646/bijbnt.001
www.bohrpub.com

A Model for Nano-Scale Spherical Surface Coverage and Protein Corona Formation By Amyloidogenic Peptides

Kazushige Yokoyama[1,*] **and Akane Ichiki**[1,2]

[1]*Department of Chemistry, The State University of New York Geneseo College,Geneseo, NY, USA*
[2]*Center for iPS Cell Research and Application, Kyoto University, Kyoto Japan*
[*]*Corresponding author: yokoyama@geneseo.edu*

Abstract. The conformation of three amyloidogenic peptides; amyloid beta 1–40 ($A\beta_{1-40}$), alpha synuclein (α-syn), and beta-2-microglobulin (β2m) are closely associated with the process of causing neurodegenerative diseases. Use of a peptide adsorbed gold nano-particle system allowed us to investigate the interactive segment of each peptide responsible for peptide-peptide networking, which is crucial to initiate the formation of an oligomer and leads to fibrillogenesis. The adsorption orientation of the amyloidogenic peptides on the nano-gold colloid spherical surface was explained by simulating how much area of the metal surface was covered by the peptides, *i.e.*, coverage ratio, Θ. The empirically extracted Θ was explained by the summation of the 1st layer and the 2nd layer with a spiking-out orientation of the prolate. Of note, the involvement of the 2nd layer was peptide type dependent. The nano-size dependence of Θ was linearly correlated with available spacing between adjacent peptides, S_d, which were approximated as prolates, For $A\beta_{1-40}$ and α-syn, the 2nd layer was more included as S_d increased. In contrast, β2m was found to gyrate over the gold surface as S_d increased, creating a partially positive ($\delta+$) region and repelling the extra β2m from the surface. Thus, as S_d decreased, it prohibited the gyration of β2m resulting in less $\delta+$ region, and more β2m monomers were adsorbed with $\delta+$ segment as the 2nd layer than the case where β2m gyrates more under relatively larger S_d. Based on the trend found in an experimentally extracted Θ as a function of S_d, optimized charge distribution of $A\beta_{1-40}$ and α-syn were concluded to be negative partial charge ($\delta-$) region that was covered by the positive partial charge ($\delta+$) region. However, β2m may have a relatively large and/or distributed $\delta+$ region with a small portion of $\delta-$ at the one end of a prolate. The characterization made in this work confirmed current understandings on the formation of the protein corona over nano-particles.

Keywords: Amyloidogenic peptides, gold nano-particles, protein folding, protein oligomerization, protein aggregation, protein corona.

INTRODUCTION

The amyloidogenic peptides are hallmarks of neurodegenerative diseases. Networking of the peptides is considered to be a critical process of the formation of fibrillogenesis [1, 2]. Although many intense studies have been conducted on the fibrils or oligomer formations of the amyloidogenic peptides, exact and clear characterization of an initial step of peptide networking has not been concluded. Neurodegenerative diseases, such as Alzheimer's disease or Parkinson's disease, are generally understood to be caused by an association of amyloidogenic peptides, such as amyloid beta 1–40 or amyloid beta 1–42 ($A\beta_{1-40}$ or $A\beta_{1-42}$), or α-synuclein (α-syn), respectively. The formation of fibrils pathologic to brain cell was known to be caused by the polymerization of an oligomer constructing the parts of a fiber (fibril). Thus, all fibrillogenesis originates from the formation of oligomers [3–7]. However, the initial formation of an oligomer needs to have an interaction between peptides, which has not been investigated in detail due to the challenge that initial oligomer formation is regarded as transient and involving very unstable intermediates.

Our group conducted a series of studies focusing on the peptide networking, which can be critical for an oligomer formation, by utilizing amyloidogenic peptides coated gold nano-colloid. The approach we took was to

prepare a peptide – coated gold-nano particle, in which a particular segment of the peptide was responsible for adsorbing onto the nano-gold surface side (presumably $\delta-$ surface). For Aβ_{1-40} the ^{28}K was assumed to be the surface contact point with the 1–27 sequence of mainly hydrophilic residues responsible for peptide-peptide interaction and networking [8]. This networking of the peptides results in aggregation of the gold colloids and allows us to probe conformation change spectroscopically as a red-shift of SPR (Surface Plasmon Resonance) from the 530 nm region when soluble to around 600 nm after aggregation. The spectroscopic investigation was combined with a control of the peptide conformation change induced by external pH change. The most plausible conformation at neutral and basic condition was estimated to be a folded conformation, while an unfolded conformation was supported at the acidic condition. The unfolded conformation permits 1–27 segments to be used for a peptide-peptide interaction resulting in a gold colloid aggregation. The observation of the SPR absorption band (λ_{peak}) as a function of pH indirectly monitors the variance of the peptide conformation change in a sigmoidal plot to extract the information of the surface property change of the gold colloid surface depending on the peptide coverage ratio, Θ [9]. This methodology was applied to investigate the adsorption orientation of the spike protein of SARS-CoV-2 coated over gold nano-particles concluding the nano-size dependence on the affinity to the gold surface [10, 11].

The coverage of proteins over nanoparticles is known as protein corona, which has been gathering an intense interest as a biomaterial in biochemical applications or for use in immunology for a material to facilitate cell-uptake. Thus, investigation of physicochemical characterization of the protein corona due to conformational change (*i.e.*, folding or unfolding) is extremely critical to understand the aggregation process [12–15]. A formation of protein corona is considered to be initiated by an adsorption under equilibrium with free proteins. A general consensus on a protein corona is that it consists of hard and soft protein corona depending on its affinity to the nano-particles' surfaces [16]. The protein corona of amyloidogenic peptides to the gold nano-particles have not been fully investigated since the focus for the amyloidogenic peptides have been toward to the end product of fibrillogenesis (amyloids). The amyloidogenic peptide coated gold nano-particles allowed to investigate the initial protein networking crucial for fibrillogenesis, since the gold nano-particles act as an inhibitor preventing further protein-protein networking. Thus, the amyloidogenic peptides coated gold colloid potentially reveals the plausible adsorption orientation and an interfacial structure as they form gold colloid aggregates.

As a crucial step for designing biomaterials, the adsorption orientation of a protein at the nano-interface has been gaining much attention [17–20]. The adsorption orientation was determined to be "spiking-out", as opposed to the "lie-down" orientation, which possesses more contacting area. The spiking-out orientation was used to extract the peptide coverage ratio (Θ) and the empirical method was justified using the simulation with the spiking-out orientation. The Θ was not exhibiting a monotonic feature as a function of gold-colloid diameter (d). While our simulation adopted a simplification in the protein structure as a prolate top, the reproduction the observed Θ extracted the possible geometrical parameter. It was found that the explanation of Θ was fully verified by involving the 1st and the 2nd layer, while no exact reasoning of the Θ for a given d [9]. This work attempted to explain any logical source relating Θ and the determining parameter. The Θ was approximated to be significantly determined by the 2nd layer involvement. The positioning of each prolate is hypothesized to be equally placed at the equatorial belt with a spacing distance between two adjacent prolates, S_d. The Θ value, therefore, was examined by utilizing the correlation to S_d.

EXPERIMENTAL

Materials and Procedure

The details of concentration of three amyloidogenic peptides used in this work – Aβ_{1-40} peptide (MW; 4.2 kDa, r-Peptide (Bogart, GA, USA)), α-syn (MW: 14.4 kDa, r-Peptide (Bogart, GA, USA)), and β2m (MW: 12 kDa/mol, AbD Serotec (Raleigh, NC, USA)) – were described elsewhere and a brief description will be given [21, 22]. Gold nanoparticles (Ted Pella, Inc. (Redding, California, USA)) were prepared with the following estimated diameters (d, nm) and reported diameter (d, nm) and particle numbers in mL: $d = 10(d = 9.8 \pm 1.0, 1.4 \times 10^{12})$, $d = 15(d = 15.2 \pm 1.5, 2.8 \times 10^{11})$, $d = 20(d = 19.7 \pm 1.1, 1.4 \times 10^{11})$, $d = 30(d = 30.7 \pm 1.3, 4.0 \times 10^{10})$, $d = 40(d = 40.6 \pm 1.1, 1.8 \times 10^{10})$, $d = 50(d = 51.5 \pm 4, 8.2 \times 10^{9})$, $d = 60(d = 60 \pm 1.0, 4.3 \times 10^{9})$, $d = 80(d = 80 \pm 1.0, 2.2 \times 10^{9})$, and $d = 100(d = 99.5 \pm 1.3, 1.6 \times 10^{9})$. The formation of the amyloidogenic peptides (Aβ_{1-40}, α-syn, and β2m) – coated gold nano-particles was conducted by mixing gold nano-particles ranging from $d = 10$ nm to 100 nm to peptides with the ratio between all peptides ($\sim$300 pM) and gold nanoparticles set as $\sim$500:1. The pH range of the solutions (between pH 2 and $\sim$pH 7) was achieved by adding hydrochloric acid (HCl) to adjust pH value gradually up to pH 2 under the constant temperature $25 \pm 0.5^{\circ}$C. The UV–V is absorption spectra were monitored between 400 nm and 850 nm as the pH value varied by an increment of 0.1 ± 0.05 to the pH of acidic conditions focusing on the red shift of SPR (surface plasmon resonance) band, which is sensitive to the formation of gold colloid aggregates.

Data Process and Analysis

The data analysis process of each absorption spectrum and procedures for extracting surface coverage ratio (Θ) was described in detail in previous publication [8]. Here, a brief description of the process will be given. All observed absorption spectra were fit by the "Peak Fit" program in Origin (Version 9.5, Originlab Corporation, Northampton, MA, USA) and the average peak position, λ_{peak}(pH), of the SPR band at given pH was extracted to construct a sigmoidal plot. The all-simulation process to extract the surface coverage ratio (Θ) and the calculation and optimization of the adjacent distance (S_d) of prolate model were completed by utilizing the process described in the section below.

RESULTS

In this study, a shift of the average peak shift at given pH, λ_{peak}(pH), was examined as a function of pH change. The λ_{peak} was extracted by weighting the area of each peak component expressed by a Gaussian profile. The plot of λ_{peak} as a function of an externally controlled pH value exhibited a sigmoidal feature described by Boltzmann Model shown in Eqn. (1).

$$\lambda_{peak}(\mathrm{pH}) = [\lambda_{\min} - \lambda_{\max}]/\{1 + \exp[(\mathrm{pH} - \mathrm{pH}_o)/d\mathrm{pH}]\} + \lambda_{\max} \quad (1)$$

Here, pH_o corresponds to an inflection point of a sigmoidal curve, and the minimum and maximum of the λ_{peak} was given by the $\lambda_{\min}$ and $\lambda_{\max}$, respectively. They have the relationship at pH_o as given in Eqn. (2).

$$\lambda_{peak}(\mathrm{pH}_o) = (\lambda_{\min} + \lambda_{\max})/2 \quad (2)$$

The $\lambda^{(1)}_{peak}$ is the first derivative of the λ_{peak}(pH), and dpH is defined as:

$$d\mathrm{pH} = (\lambda_{\max} - \lambda_{\min})/4\lambda^{(1)}_{peak} \quad (3)$$

There is one empirically extracted premise, which was used to establish $\Theta_{\exp}$ (*i.e.*, experimentally extracted surface coverage ratio). The $\Delta\mathrm{pH}_o$ is defined as pH_o (amyloidogenic peptide-coated gold colloid, d nm) – pH_o (bare gold, d nm), and was found to be linearly correlated with $1/\lambda^{(1)} \propto d\mathrm{pH}$ as

$$d\mathrm{pH} = \alpha\Delta\mathrm{pH}_o + \beta \quad (4)$$

Here, α and β are a slope and an x-axis intercept. The $\Delta\mathrm{pH}_o$ was confirmed as it was directly related to the peptide coverage fraction, Θ, thus, $\Delta\mathrm{pH}_o = 0$ corresponds to $\Theta = 0$ (*i.e.*, no peptide coverage or bare gold colloid), and the x-axis intercept of the Eqn. (4) corresponds to the maximum value of $\Delta\mathrm{pH}_o$ and $\Theta = 1$, as shown in Fig. 1. Therefore, any Θ values in between $\Delta\mathrm{pH}_o = 0$ and $\Delta\mathrm{pH}_o(\mathrm{max.})$ are given by Eqn. (5).

$$\Theta = \frac{\Delta\mathrm{pH}_o}{\Delta\mathrm{pH}_o(\mathrm{max})} \quad (5)$$

Here, $\Delta\mathrm{pH}_o(\mathrm{max}) = -\beta/\alpha$. Since there was no clear correlation between Θ and d, we attempted to find another parameter, which controlled Θ. The total Θ was estimated to be a sum of Θ(1st layer) and Θ(2nd layer). On the average 29% (Aβ_{1-40}), 42% (α-syn), and 32% (β2m) of total Θ was constructed from the 2nd layer. After the Θ(1st layer) was maximized, Θ(2nd layer) would be optimized by the spacing between two adjacent prolates, S_d, created by the prolates in the 1st layer (See Fig. 2). First, the maximum number of prolates to be positioned on the equatorial circumference (n_{eq}) without overlapping each other (*i.e.*, $S_d > 0$) was calculated as:

$$S_d = \frac{2\pi r - 2an_{eq}}{n_{eq}} = \frac{\pi d - 2an_{eq}}{n_{eq}} \quad (6)$$

For example, the optimized axial length of the prolate exhibited for Aβ_{1-40} was $a = 1.4$ nm and $b = 2.2$ nm. The n_{eq} for the gold colloid 15 nm and 30 nm was 21

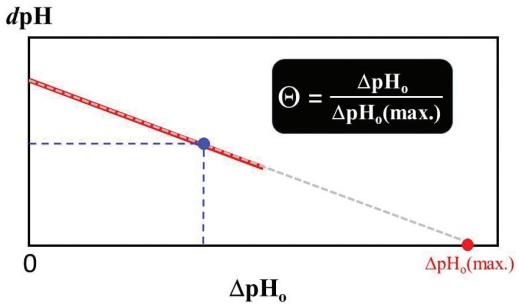

Figure 1. A sketch illustrating the extraction of the coverage ratio (Θ) from the linear relationship between dpH vs. $\Delta\mathrm{pH}_o$ as given in Eqn. (4). There was no correlation between the gold colloidal size and its coverage ratio of peptide (Θ) found in our study.

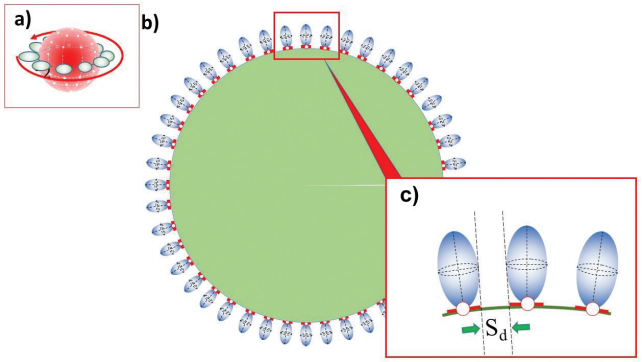

Figure 2. a) The sketch of prolates locating over a spherical surface found in an equatorial belt and b) its blow-up (and bird's eye view). c) The S_d was indicated as an adjacent distance between two prolates.

Table 1. The resulting S_d value, the optimized gold nano-particle diameter (ξ nm) and the axial lengths (a and b) of a prolate for optimizing Θ vs. S_d plot (*i.e.*, $\Theta = \phi\ S_d + \epsilon$) for a) A$\beta_{1-40}$, b) α-syn., and c) β2m corresponding to the plot in Figures 3 a)–c), respectively. Here, d is the actual reported value of each gold [23].

a) Aβ_{1-40}

d (nm)	ξ (nm)	$\xi - d$ (nm)	$d\xi$ (%)	a (nm)	b (nm)	Θ	S_d(pm)
9.8	10.057	0.257	2.6	2.199	1.400	0.6195	38.23
15.2	14.895	−0.305	−2.0	2.077	1.400	0.8098	49.72
19.8	20.044	0.244	1.2	2.201	1.400	0.7213	44.42
30.7	30.903	0.203	0.7	2.185	1.400	0.6745	41.37
40.6	39.193	−1.407	−3.6	2.181	1.400	0.8319	50.67
51.5	51.578	0.078	0.2	2.202	1.400	0.5929	36.66
60.0	60.624	0.624	1.0	2.203	1.400	0.6018	37.47
80.0	80.27	0.27	0.3	2.200	1.400	0.7448	29.77
99.5	99.422	−0.078	−0.1	2.200	1.400	0.1902	11.78
Avg.			0.026				

b) α-syn

d (nm)	ξ (nm)	$\xi - d$ (nm)	$d\xi$ (%)	a (nm)	b (nm)	Θ	S_d(pm)
9.8	9.430	−0.37	−4.1	7.399	4.600	0.5387	314
15.2	15.763	0.563	4.2	7.398	4.600	0.6469	400
19.8	18.639	−1.161	−5.6	7.399	4.600	0.5926	350
30.7	31.185	0.485	0	7.400	4.600	0.6745	431
40.6	37.911	−2.689	−0.3	7.401	4.600	0.1543	0.154
51.5	51.535	0.035	0	7.400	4.600	0.4896	273
60.0	60.215	0.215	1.0	7.400	4.600	0.4386	227
80.0	81.838	1.838	2.2	7.400	4.600	0.5782	287
99.5	96.481	−3.019	−0.03	7.400	4.600	0.6685	249
Avg.			−0.28				

c) β2m

d (nm)	ξ (nm)	$\xi - d$ (nm)	$d\xi$ (%)	a (nm)	b (nm)	Θ	S_d(pm)
9.8	9.181	−0.619	−6.7	4.600	2.500	0.4716	250
15.2	15.204	0.004	0.03	4.600	2.500	0.7540	111
19.8	20.955	1.155	5.5	4.600	2.500	0.4409	263
30.7	31.348	0.648	2.1	4.600	2.500	0.7887	95.4
40.6	41.286	0.686	1.7	4.599	2.500	0.7473	116
51.5	52.696	1.196	2.3	4.600	2.500	0.7473	117
60	60.828	0.828	1.4	4.600	2.500	0.4735	116
80	80.838	0.838	1.0	4.600	2.500	0.8850	51.1
99.5	99.026	−0.474	−0.5	4.600	2.500	0.9902	2.951×10^{-2}
Avg.			+0.75				

and 39, respectively. The estimated Θ achieved by the 1st layer was 46% for both 15 nm and 30 nm. The optimized S_d value for 15 nm and 30 nm gold colloid was found to be 49.7 pm and 41.37 pm, (See Table 1) indicating that 30 nm gold colloid possesses the smaller S_d resulting in less involvement of the 2nd layer. The $\Theta_{total}(15\ \text{nm}) = 0.8098$ and $\Theta_{total}(30\ \text{nm}) = 0.6745$ and confirmed that S_d (15 nm) $>$ S_d (30 nm) causing $\Theta(15\ \text{nm}) > \Theta(30\ \text{nm})$ due to a significant contribution from the 2nd layer.

The Θ was approached by hypothesizing the S_d correlation in Eqn. (7).

$$\Theta = \phi S_d + \epsilon \tag{7}$$

A predicted correlation between Θ and S_d was confirmed for Aβ_{1-40} and α-syn (Fig. 3a, a′, b, and b′), where $\phi > 0$. However, for β2m, the correlation between Θ and S_d exhibited a negative slope ($\phi < 0$) as shown in Fig. 3c and 3c′. The Θ_{obs} was analyzed by floating d transforming to ξ with predetermined prolate parameters a and b. The

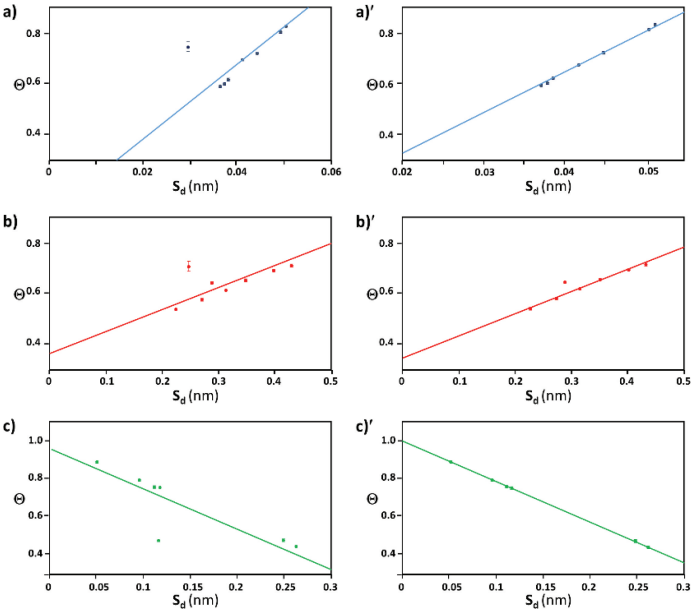

Figure 3. The best optimized plot of Θ vs. S_d for (a) Aβ_{1-40} in blue, (b) α-syn in red, and (c) β2m in green, with fitting values for the linear relationship given in Eqn. (6). Each primed figure (a′, b′, and c′) shows the plot when each outlier point was removed.

Table 2. The optimized parameters ϕ and ϵ for a formula in Eqn. (6) for a) Aβ_{1-40}, b) α-syn., and c) β2m, where fitting values for the linear relationship $\Theta = \phi\ S_d + \epsilon$. Two types of fits were conducted as, (I) the fit with all data points shown in Figures 4a)–c), and (II) the fit excluding a selected data point shown in Figures 4a)′–c)′. Here, the coefficient of the determination, $\langle R^2 \rangle$, values are also shown.

		a) Aβ_{1-40}	b) α-syn	c) β2m
(I)	ϕ	15(3)	1.2(2)	−2.0(4)
	ϵ	0.1(1)	0.20(6)	0.95(6)
	$\langle R^2 \rangle$	0.8024	0.8135	0.7812
(II)	ϕ	16.4(1)	1.22(8)	−2.082(9)
	ϵ	−0.007(6)	0.17(2)	0.989(1)
	$\langle R^2 \rangle$	0.9996	0.9763	0.9998

optimized parameters are summarized in Table 2. In spite of variation of all parameters, we found one data point which deviated from the predicted trend, and they were $d = 80$ nm for Aβ_{1-40}, $d = 80$ nm for α-syn, and $d = 60$ nm for β2m. Each primed Fig. 3a′–c′ show the plot when each outlier point was removed. The discovered Θ indicated the relatively high values and that a spiking-out orientation was required in order to achieve this Θ value.

DISCUSSION

The empirically extracted surface coverage ratio, Θ, of amyloidogenic peptides over the nano-gold colloid was explained by the distance between two adjacent prolates, S_d. The S_d significantly influenced the intrusion of the 2nd layer of the peptide. However, the sign of the linear correlation depended on the peptide. As the S_d increased,

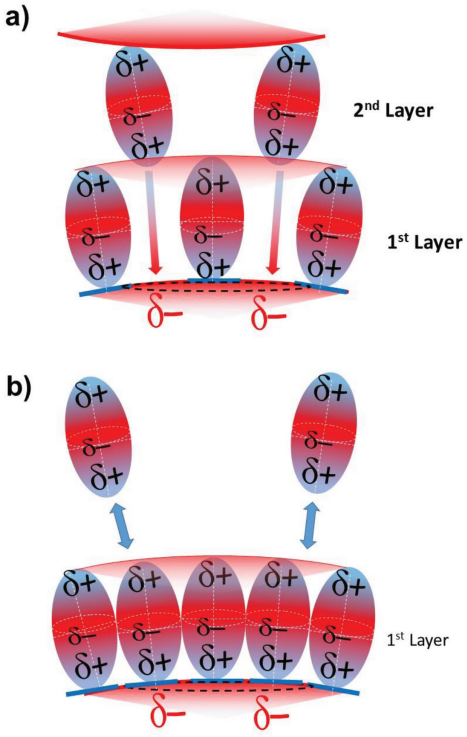

Figure 4. A sketch indicating the second layer was relatively easily invited in for the case of a prolate possessing the $\delta+$ at the bottom of a prolate a). On the other hand, smaller S_d repels the incoming second layer b).

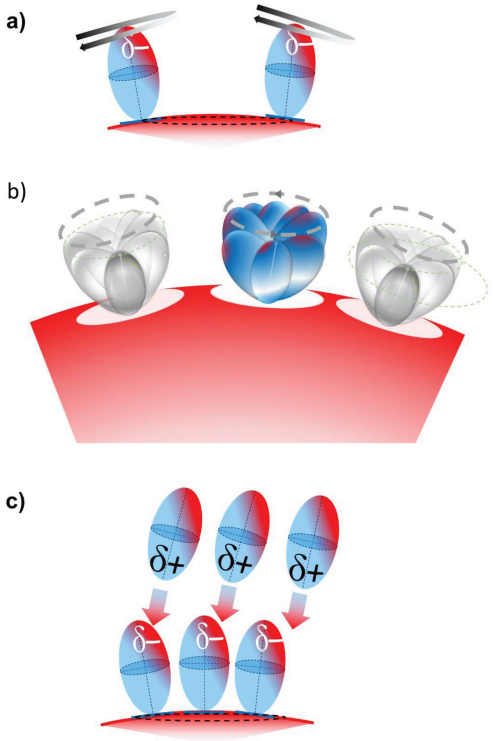

Figure 5. a) The relatively larger S_d allows a prolate to gyrate resulting in exposing $\delta+$ field and repelling the approaches of the second layer as shown in b). c) The relatively smaller S_d does not allow the prolate to gyrate and fixed in the location instead exposing $\delta-$ region attracting $\delta+$ of the second layer to approach.

the area of gold colloidal surface with $\delta-$ distribution must be more exposed to the 2nd layer. For Aβ_{1-40} and α-syn, an increase of S_d worked out favorably to invite more 2nd layer and leading to the higher Θ. In contrast, an increase of S_d with β2m reduced the involvement of the 2nd layer and resulted the lower Θ. This opposite trend with β2m is attributed to a partial charge distribution of each amyloidogenic peptide, where peptide shape was simplified as a prolate. Placing a model prolate in a spiking out adsorption orientation, the bottom side with $\delta+$ became a contacting point for an adsorption. If the decrease of S_d prohibits an increase of Θ (invitation of the 2nd layer), the top portion of a prolate must possess $\delta+$, so that a middle region (or an equatorial belt area) of a prolate should thus possess a $\delta-$ charge (Fig. 4a and 4b). The previous study concluded that hydrophobic segment was responsible for contacting on the gold surface [23]. Hypothesizing that $\delta+$ region in the hydrophobic region was responsible for the adsorption, lysine 28 (^{28}K) for Aβ_{1-40} and lysines 80, 96, and 97 (^{80}K or ^{96}K^{97}K) for α-syn| was considered to be responsible for an adsorption on the gold colloid surface. As for $\delta+$ region of the hydrophilic side of Aβ_{1-40}, the 5th Arginine and 6th Histidine (^{5}R^{6}H), 13th and 14th Histidine (^{13}H^{14}H), or 16th Lysine (^{16}K) were plausible positively charged residues. As for α-syn, all Lysine in the 6, 10, 12, 21, 23, 32, and 34 sequences were speculated to be $\delta+$ region of the hydrophilic (N-terminal) side.

In order to explain the opposite trend found in Θ vs. S_d (Fig. 3c and 3c′), the partial charge distribution over a prolate surface was estimated to be dominated by $\delta+$ as shown in Fig. 5. Since β2m tended to gyrate as more surface area was available (as S_d increased), an extra β2m monomers were less invited due to predominant $\delta+$ surface potential. While the $\delta-$ portion adsorbed on the other gold nan-particles, thus the orientation flip may not occur (Fig. 5a). On the other hand, a relatively smaller S_d constrain a degree of freedom giving less degree of freedom prohibiting gyration and facilitating $\delta-$ to be attracted to $\delta+$ region. (See Fig. 5c) The 63rd Arginine (^{63}R), 66th Lysine (^{66}K) or 69th Histidine (^{69}H) at the C-terminal side of β2m were estimated to be used for the adsorption site. As for the $\delta-$ region near N-terminal side, glutamic acid 18 (^{18}E) was proposed as the negatively charged residue.

Our present work provides a geometry and charge based model that helps explain hard and soft protein corona formation on a metal nanoparticle surface. The adsorption of the mobile protein with many binding sites to nanoparticles with different affinities is considered to be an initial stage (*i.e.*, Vrom, then an effect) [24] under the diffusion dominated condition, relatively lower affinity proteins adsorbed first, then followed by a replacement by relatively slower diffusing and higher affinity proteins [25] with relatively lower activation energies [16].

Current work strongly suggests that protein corona formation and its coverage strongly depend on nano-particle (core) size. The formation of the gold aggregates indicates that protein conformation of the corona can be controlled by an external pH change transforming unfolded proteins and constructing a protein-protein networks to form gold aggregates. The hard corona can be identified as the 1st layer in this work, and the soft corona can be identified as the 2nd layer (*i.e.*, the peptides adsorbed on the other surrounding gold colloids). Our recent study showed that the formation of the aggregates did not depend on surface coverage but rather affected by the core size of gold particle and indicating the formation of soft corona is more dominated by physical spacing available for the protein-protein interaction [26]. The adsorption orientation was concluded to be as spiking out orientation, which is in good agreement with the Stellacci group's reports of co-polymer adsorbed on the metal nanoparticles [27–29]. A recent study using Molecular Dynamics simulations by Pranab Sarker *et al.* [30] reported that bare silver nanoparticles interact with ovispirin-1 peptides exhibiting surface hydrophilicity effects on formation dynamics and the construction and structure of the peptide corona. An entire adsorption process on silver nanoparticle surfaces was generalized by diffusion landing *via* hydrophilic residues most likely through a Lysine, which was a good agreement with our hypothesis. However, the orientation of the protein was predicted to be depending on the nano size and a lying down orientation was plausible for the 10 nm diameter silver particle while no particular preference was found for the 3 nm diameter silver particles [30].

The most significant outcome of this work was the rationalization of the relationship between Θ and the gold colloidal size diameter (d). The description of Θ was found not to be a monotonic function of the gold diameter. Based on the fact that Θ was explained by S_d, the relationship between Θ and d can be reduced to a complex function as shown in Eqns. (8)–(11) for the case of $a > b$.

$$S_d = \frac{L_A - L_F}{n_{eq}} = \frac{d + 2b\pi}{\left\lfloor \frac{\pi\left(\frac{d}{2}+a\right)}{a} \right\rfloor} - 2a \tag{8}$$

$$L_A = d + 2a\pi \tag{9}$$

$$L_F = 2bn_{eq} \tag{10}$$

$$n_{eq} = \left\lfloor \frac{\pi\left(\frac{d}{2}+a\right)}{a} \right\rfloor \tag{11}$$

Substituting Eqn. (8) into Eqn. (7),

$$\Theta = \phi \left\{ \frac{d + 2b\pi}{\left\lfloor \frac{\pi\left(\frac{d}{2}+a\right)}{a} \right\rfloor} - 2a \right\} + \epsilon \tag{12}$$

The 1st term in S_d expression is not a monotonic function of d. The Fig. 6 clearly shows the undulation of the S_d value while the worked d value was limited to those shown in Table 1. Thus, the optimized S_d requires to be adjusted to be ξ as shown in Table 1.The value ξ can be interpreted as two ways. First, ξ can be recognized as the actual d value in the prepared sample, and this is the value to be considered as a reporting value for the diameter of the gold particles. The difference between ξ and d was found to be within ∼7%, indicating a reasonable matching between the reported values, considering that maximum distribution in the reported value was almost ∼10%. The second interpretation of ξ can be an effective diameter as the peptide was surrounded, or when the surface of gold was hydrated. When $\xi < d$, it shows that the surface area was strongly attracted by the peptides showing the expansion. On the other hand, $d > \xi$ case can be regarded as an opposite effect of the previous case where the gold surface experienced a strong repulsion from the peptide. Following the above hypothesis, Aβ_{1-40} may not affect the gold surface electrostatically. However, α-syn must be repulsively interacting with the gold surface, reducing the effective gold colloidal size, while β2m must be more attractive to the gold colloidal surface. It was interpreted that the overall effective surface charge of the area (segments) of β2m was used for the adsorption.

The off-trend points observed in S_d and $d(\xi)$ relationship in Figs. 3a, 3b, and 3c, were at d^* (Aβ_{1-40}) = 80 nm for Aβ_{1-40} at S_d = 29.77 pm, d^* (α-syn) = 80 nm for α-syn at S_d = 287 pm, d^* (β2m) = 60 nm for β2m at S_d = 116 pm, respectively as shown in Table 1. Under d^* (Aβ_{1-40}) and d^* (α-syn), significantly higher Θ values were observed than what trend predicted by the rest. On the other hand, significantly lower Θ was observed at d^* (β2m) than what the trend predicted. These off-trend points at d^* were considered as a result of break-down of approximation made in Eqn. (7), where a physical spacing between two adjacent prolates (S_d) with an angle were only used as a determining factor of a coverage with a spiking out orientation with a long molecular axis normal to the surface. Thus, ξ adjusts the discrepancies between pure physical model based on only S_d and the secondary term coming from intermolecular forces which were completely ignored in Eqn. (7). Therefore, three Θ values observed at d^* must imply a significant contribution of intermolecular forces not being ignored at particular S_d. Generally speaking, the potential of two dipole-dipole potential created by two dipoles A and B by end-to-end formation is given in Eqn. (13):

$$V(r) = -\frac{\mu_A \mu_B}{4\pi\varepsilon_o r_{AB}^3}(\cos\theta_{AB} - 3\cos\theta_A \cos\theta_B) \tag{13}$$

Here, μ is a dipole moment, ϵ_o is the permeability of space, θ_{AB} is the angle made by the two dipoles, r_{AB} is the distance between the two dipoles A and B. Also, θ_A and θ_B

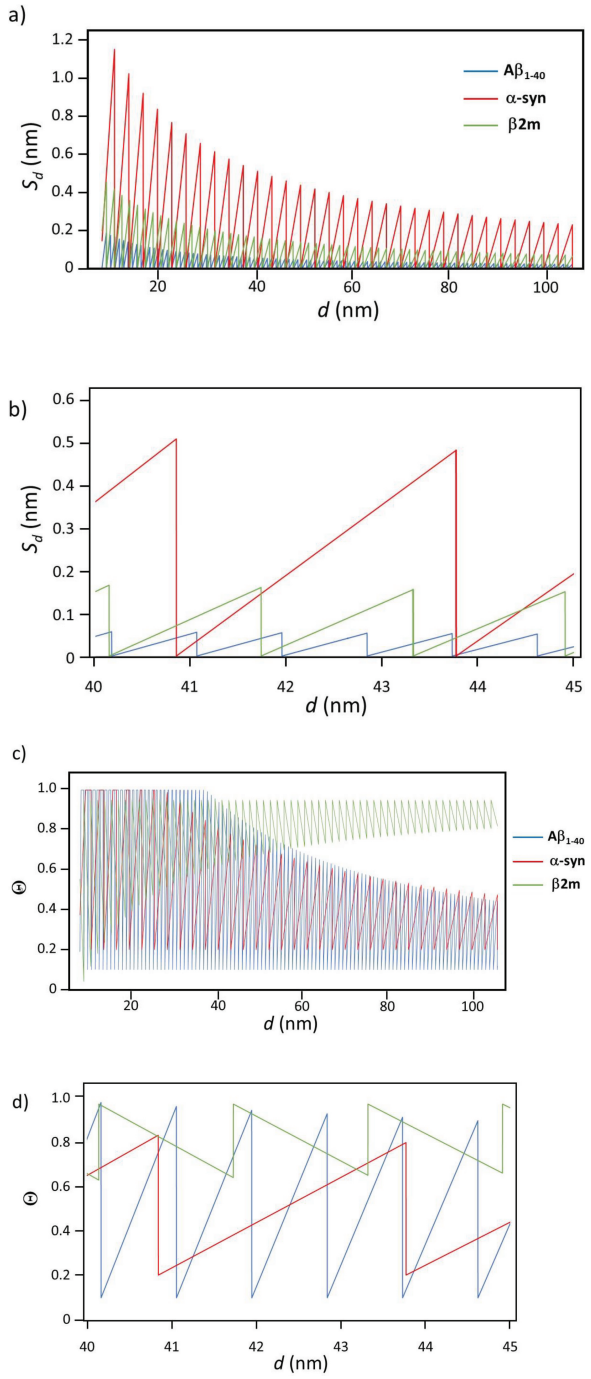

Figure 6. a) The simulation of S_d as a function of d by using Eqn. (8) with a and b listed in Table 1 for Aβ_{1-40}: blue, α-syn: red, and β2m: green. b) A blow up in the range between d = 40 and 45 nm. c) The simulation reproducing Θ as a function of colloidal diameter, d, using Eqn. (12) with parameters listed in Table 2 (II). d) The Θ vs. d plot given for the region between 40 and 45 nm.

are the angles formed by the two dipoles with respect to the line connecting their centers. Because present alignment of the dipoles is placed tandemly on the surface θ_A or θ_B are not well defined. The $\delta+$ region of the peptides must not be distributed concentrically requiring the tilting angle of the adsorption (*i.e.*, the spiking-out orientation angle is not normal to the adsorption surface). The tilting angle must be varied depending on the S_d and hypothesized as a quadratic or higher order function of S_d. Assuming Aβ_{1-40} and α-syn could produce minimum potential energy at tilting angle was minimized (*i.e.*, no tilting) and β2m minimizes the potential at the maximum tilting angle (*i.e.*, almost lie-down formation at each S_d under specific d^*). For Aβ_{1-40} and α-syn, the minimum tilting angle minimize the exposure of the $\delta+$ region resulting in more invitation of the second layer by attracting $\delta+$ of the guest prolate (2^{nd} layer) to their $\delta-$ of the 1^{st} layer. Reversely, at d^* the β2m must maximize the $\delta+$ region with gyrational motion and invited the 2^{nd} layer causing less Θ.

CONCLUSIONS

The surface coverage ratio of the amyloidogenic peptides over the nano-gold colloid was approached with a physical hypothesis of the adjacent distance of the peptides, which were approximated to be prolates in this study. The Aβ_{1-40} and α-syn exhibited the more involvements of the second layer causing the higher theta as the available Sd increased. On the other hand, β2m increased theta as the S_d decreased. The correlation between theta and S_d was explained by the partial charge distribution over the prolate surface, where Aβ_{1-40} (and α-syn) possessing $\delta+$ at both ends of axial positions. This allows these peptides to exhibit more $\delta-$ to invite in the second layer as S_d increases. The major partial charge of β2m, on the other hand, the proposed to be covered by a $\delta+$. As the S_d increases, β2m was able to explain theta by making S_d to gyrate creating a wide area of partially positive region and inhibiting the second layer to participate. The physical and mathematical approach was able to explain theta by a unique step function of the diameter, d, of the gold colloid, and the opposite trend in a different peptide required a reasoning of a partial charge distribution hinting the structural information of the adsorbed peptides. This work provides a simplified geometric and partial charge based model that accounts for amino acid general physicochemical character to help elucidate peptide-metal adsorption and nanoparticle corona formation.

ACKNOWLEDGEMENTS

We are grateful for the support provided by the Geneseo Foundation at the initial stages of this project. Akane Ichiki is thankful for the gracious support from the SUNY Geneseo Chemistry Department Alumni Summer Research Scholarship and Dreyfus Foundation Undergraduate Summer Research Scholarship. We also thank Jonathan Bourne for helpful discussion during the preparation of this manuscript.

REFERENCES

[1] D.M. Walsh, A. Lomakin, G.B. Benedek, M.M. Condron, D.B. Teplow, Amyloid-protein fibrillogenesis, J. Biol. Chem., 272 (1997) 22364–22372.

[2] A. Lomakin, D.S. Chung, G.B. Benedek, D.A. Kirshner, D.B. Teplow, On the nucleation and growth of amyloid-protein fibrils: detection of nuclei and quantitation of rate constants, Proc. Natl. Acad. Sci. USA., 93 (1996) 1125–1129.

[3] A. Moshe, M. Landau, D. Eisenberg, Preparation of Crystalline Samples of Amyloid Fibrils and Oligomers, Methods Mol Biol., 1345 (2016) 201–210.

[4] R. Pujol-Pina, S. Vilapriny-Pascual, R. Mazzucato, A. Arcella, M. Vilaseca, M. Orozco, N. Carulla, SDS-PAGE analysis of Aβ oligomers is disserving research into Alzheimer's disease: appealing for ESI-IM-MS, Sci Rep, 5 (2015) 14809–14821.

[5] W. Paslawski, M. Andreasen, S.B. Nielsen, N. Lorenzen, K. Thomsen, J.D. Kaspersen, J.S. Pedersen, D.E. Otzen, High Stability and Cooperative Unfolding of α-Synuclein Oligomers Biochemistry, 53 (2014) 6252–6263.

[6] G. Comellas, L.R. Lemkau, D.H. Zhou, J.M. George, C.M. Rienstra, Structural Intermediates during α-Synuclein Fibrillogenesis on Phospholipid Vesicles, J. Am. Chem. Soc., 134 (2012) 5090–5099.

[7] G. Esposito, M. Garvey, V. Alverdi, F. Pettirossi, A. Corazza, F. Fogolari, M. Polano, P.P. Mangione, S. Giorgetti, M. Stoppini, A. Rekas, V. Bellotti, A.J.R. Heck, J.A. Carver, Monitoring the Interaction between Beta2-Microglobulin and the Molecular Chaperone alpha B-crystallin by NMR and Mass Spectrometry : alpha B-Crystallin dissociates Beta 2-Microglobulin Oligomers, The Journal of Biological Chemistry, 288 (2013) 17844–17858.

[8] K. Yokoyama, K. Brown, P. Shevlin, J. Jenkins, E. D'Ambrosio, N. Ralbovsky, J. Battaglia, I. Deshmukh, A. Ichiki, Examination of Adsorption Orientation of Amyloidogenic Peptides Over Nano-Gold Colloidal Particles' Surfaces, International Journal of Molecular Science, 20 (2019) 5354–5380.

[9] K. Yokoyama, A. Ichiki, Oligomerization and Adsorption Orientation of Amyloidogenic Peptides over Nano-Gold Colloidal Particle Surfaces, in: J.C. Taylor (Ed.) Advances in Chemical Research, NOVA Science Publisher, Hauppauge, NY, USA., 2020, pp. 139–194

[10] K. Yokoyama, A. Ichiki, Nano-size dependence in the adsorption by the SARS-CoV-2 spike protein over gold colloid, Colloids and Surfaces A: Physicochemical and Engineering Aspects, 615 (2021) 126275–112681.

[11] K. Yokoyama, A. Ichiki, Spectroscopic Investigation on the Affinity of SARS-CoV-2 Spike Protein to Gold Nano-Particles Colloid and Interface Science Communication, 40 (2021) 100356–100362.

[12] N. Hooshmand, A. Thoutam, M. Anikovskiy, H.I. Labouta, M. El-Sayed, Localized Surface Plasmon Resonance as a Tool to Study Protein Corona Formation on Nanoparticles, J. Phys. Chem. C 125 (2021) 24765–24776.

[13] M. Rahman, S. Laurent, N. Tawil, L.H. Yahia, M. Mahmoudi, Protein-Nanoparticle Interactions, The Bio-Nano Interface; Springer, Springer 2013, pp. 21–44.

[14] M. Lundqvist, I. Sethson, B.-H. Jonsson, Protein Adsorption onto Silica Nanoparticles: Conformational Changes Depend on the Particles' Curvature and the Protein Stability, Langmuir 20 (2004) 10639–10647.

[15] J. Wolfram, Yong Yang, Jianliang Shen, Asad Moten, Chunying Chen, Haifa Shen, Mauro Ferrari, Y. Zhao, The nano-plasma interface: Implications of the protein corona Colloids Surf., B 124 (2014) 17–24.

[16] V.P. Zhdanov, B. Kasemo, Monte Carlo simulation of the kinetics of protein adsorption. Proteins: Struct. Funct. Genet., 30 (1998) 177–182.

[17] L. Filali, Y. Brahmi, J.D. Sib, Y. Bouizem, D. Benlakehal, K. Zellama, N. Lemée, A. Bouhekka, F. Kail, A. Kebab, L. Chahed, Local Surface Electric Field's Effect on Adsorbed Proteins' Orientation Surfaces, (2019) 415–431.

[18] B.E. Givens, N.D.F. Diklich, J.; Grassian, V.H. Adsorption of bovine serum albumin on silicon dioxide nanoparticles: Impact of pH on nanoparticle–protein interactions. Biointerphases 2017, 12, 02D404.

[19] J. Meissner, A. Prause, B. Bharti, G.H. Findenegg, Characterization of protein adsorption onto silica nanoparticles: Influence of pH and ionic strength, Colloid Polym. Sci., 293 (2015).

[20] A.C. McUmber, T.W. Randolph, D.K. Schwartz, Electrostatic Interactions Influence Protein Adsorption (but Not Desorption) at the Silica-Aqueous Interface., J. Phys. Chem. Lett., 6 (2015) 2583–2587.

[21] K. Yokoyama, Nanoscale Protein Conjugation in: E.J. Chen, N. Peng (Eds.) Advances in Nanotechnology Vol. 1 Nova Science Publishing 2010, pp. 65–104.

[22] K. Yokoyama, Modeling of Reversible Protein Conjugation on Nanoscale Surface in: S.M. Musa (Ed.) Computational Nanotechnology: Modeling and Applications with MATLAB, CRC Press 2011, pp. 381–409.

[23] K. Yokoyama, K. Brown, P. Shevlin, J. Jenkins, E. D'Ambrosio, N. Ralbovsky, J. Battaglia, I. Deshmukh, A. Ichiki, Examination of Adsorption Orientation of Amyloidogenic Peptides Over Nano-Gold Colloidal Particles' Surfaces International Journal of Molecular Science, 20 (2019) 5354–5380.

[24] L. Vroman, Effect of Adsorbed Proteins on the Wettability of Hydrophilic and Hydrophobic Solids Nature 196 (1962) 476–477.

[25] P. Vilaseca, K.A. Dawson, G. Franzese, Understanding and modulating the competitive surface-adsorption of proteins through coarse-grained molecular dynamics simulations, Soft Matter, 9 (2013) 6978–6985.

[26] K. Yokoyama, A. Ichiki, K. Hausrath, S. Hamazaki, I. Deshmukh, D. Akanonu, T. Lam, Nano-size dependence in aggregation process of beta 2 microglobulin coated gold colloids, Molecules, (to be submitted).

[27] A. Verma, O. Uzun, Y. Hu, Y. Hu, H.-S. Han, N. Watson, S. Chen, D.J. Irvine, F. Stellacci, Surface-structure-regulated cell-membrane penetration by monolayer-protected nanoparticles, Nature Materials, 7 (2008) 588–595.

[28] J. Yuan, X. Liu, O. Akbulut, J. Hu, S.L. Suib, J. Kong, F. Stellacci, Superwetting nanowire membranes for selective absorption, Nature Nanotechnology, 3 (2008) 332–336.

[29] K. Voïtchovsky, J.J. Kuna, S.A. Contera, E. Tosatti, F. Stellacci, Direct mapping of the solid–liquid adhesion energy with subnanometre resolution, Nature Nanotechnology VOL 5 (2010) 401–405.

[30] P. Sarker, M.S.J. Sajib, X. Tao, T. Wei, Multiscale Simulation of Protein Corona Formation on Silver Nanoparticles: Study of Ovispirin-1 Peptide Adsorption, Journal of Physical Chemistry B, 126 (2022) 601–608.